



Aligned natural–synthetic polyblend nanofibers for peripheral nerve regeneration

Chun-Yang Wang^a, Kui-Hua Zhang^{b,c}, Cun-Yi Fan^{a,*}, Xiu-Mei Mo^b, Hong-Jiang Ruan^a, Feng-Feng Li^a

^a Department of Orthopedic Surgery, Shanghai Sixth People's Hospital, JiaoTong University, Shanghai 200233, People's Republic of China

^b State Key Laboratory for Modification of Chemical Fibers and Polymer Materials, College of Materials Science and Engineering, Donghua University, Shanghai 201620, People's Republic of China

^c College of Biological Engineering and Chemical Engineering, Jiaxing College, Zhejiang 314001, People's Republic of China

ARTICLE INFO

Article history:

Received 14 June 2010

Received in revised form 16 August 2010

Accepted 7 September 2010

Available online 16 September 2010

Keywords:

Nerve guidance conduit

Peripheral nerve regeneration

Silk fibroin

Poly(L-lactic acid-co-ε-caprolactone)

Electrospinning

ABSTRACT

Peripheral nerve regeneration remains a significant clinical challenge to researchers. Progress in the design of tissue engineering scaffolds provides an alternative approach for neural regeneration. In this study aligned silk fibroin (SF) blended poly(L-lactic acid-co-ε-caprolactone) (P(LLA-CL)) nanofibrous scaffolds were fabricated by electrospinning methods and then reeled into aligned nerve guidance conduits (NGC) to promote nerve regeneration. The aligned SF/P(LLA-CL) NGC was used as a bridge implanted across a 10 mm defect in the sciatic nerve of rats and the outcome in terms of regenerated nerve at 4 and 8 weeks was evaluated by a combination of electrophysiological assessment and histological and immunohistological analysis, as well as electron microscopy. The electrophysiological examination showed that functional recovery of the regenerated nerve in the SF/P(LLA-CL) NGC group was superior to that in the P(LLA-CL) NGC group. The morphological analysis also indicated that the regenerated nerve in the SF/P(LLA-CL) NGC was more mature. All the results demonstrated that the aligned SF/P(LLA-CL) NGC promoted peripheral nerve regeneration significantly better in comparison with the aligned P(LLA-CL) NGC, thus suggesting a potential application in nerve regeneration.

© 2010 Acta Materialia Inc. Published by Elsevier Ltd. All rights reserved.

1. Introduction

Peripheral nerve injury that cannot be directly repaired by end to end sutures remains a significant clinical problem. The current gold standard for treating large nerve defects involves nerve autograft transfers, but they are limited by donor site morbidity, shortage of donor nerve and inadequate functional recovery [1,2]. An alternative approach is the use of a nerve guidance conduit (NGC) that could provide a pathway for nerve out-growth and also promote nerve regeneration. A number of synthetic or natural biopolymers, such as poly(L-lactic acid) (PLLA), poly(lactic-co-glycolic acid) (PLGA), poly(caprolactone) (PCL), collagen and chitosan, have been utilized to construct NGCs for nerve repair [3–7]. Although the advances are encouraging, neural regeneration achieved through these degradable NGCs is still unsatisfactory as a result of their biological or mechanical properties [8].

Nanofibrous scaffolds generated by electrospinning have gained increasing popularity in the field of tissue engineering over the past few years [9–14]. They are characterized by an extremely high porosity and surface area to volume ratio mimicking the features of the extracellular matrix (ECM) that is critical for tissue regeneration. Various synthetic or natural polymers and even mixed solu-

tions of these synthetic and natural polymers can be electrospun into nanofibers, to be used in tissue engineering applications. Moreover, aligned nanofibers can be obtained by correct choice of the collector in the electrospinning equipment. Aligned nanofibers have been shown to direct cell migration, which plays a critical role in nerve regeneration [15–17].

Recently our group has reported the development and characterization of natural–synthetic polymeric nanofibers comprised of well-blended silk fibroin (SF) and poly(L-lactic acid-co-ε-caprolactone) (P(LLA-CL)) by electrospinning [18]. Blending SF into P(LLA-CL) has proved to greatly improve the cell affinity of P(LLA-CL). In this study aligned SF/P(LLA-CL) nanofibers were fabricated by electrospinning with a rotating drum collector and then reeled on a stainless steel bar to fabricate an aligned NGC. The effect of the aligned SF/P(LLA-CL) NGC on nerve regeneration was assessed in a rat sciatic nerve injury model using electrophysiological, histological and immunohistological techniques and electron microscopy.

2. Materials and methods

2.1. Electrospinning materials

Bombyx mori silkworm cocoons were kindly supplied by Jiaxing Silk Co. Ltd. (China). A co-polymer of P(LLA-CL) (50:50) ($M_w =$

* Corresponding author. Tel.: +86 138 01832808; fax: +86 021 64701361.

E-mail addresses: fancunyi888@hotmail.com, fancunyi@smmail.cn (C.-Y. Fan).

$34.5 \times 10^4 \text{ g mol}^{-1}$), which has a composition of 50 mol.% L-lactide, was provided by Nara Medical University (Japan). 1,1,1,3,3,3,-Hexafluoro-2-propanol (HFIP) was purchased from Daikin Industries Ltd. (Japan).

2.2. Preparation of regenerated SF

Raw silk was degummed three times with 0.5 wt.% Na_2CO_3 solution at 100°C for 30 min each and then washed with distilled water. Degummed silk was dissolved in a ternary solvent system of $\text{CaCl}_2/\text{H}_2\text{O}/\text{ethanol}$ solution (mole ratio 1/8/2) for 1 h at 70°C . After dialysis through cellulose tubular membrane (250-7u, Sigma) in distilled water for 3 days at room temperature the SF solution was filtered and lyophilized to obtain regenerated SF sponges.

2.3. Preparation of aligned SF/P(LLA-CL) nanofibrous scaffolds and NGCs

Polymer solution (8% (w/v)) was prepared by dissolving SF/P(LLA-CL) blends at a weight ratio of 25:75 in hexafluoroisopropanol and stirred at room temperature for 6 h. Pure 8% (w/v) and 4% (w/v) P(LLA-CL) solutions were prepared by dissolving P(LLA-CL) in hexafluoroisopropanol and stirred at room temperature for 6 h. In previous experiments thick fibers ($>1000 \text{ nm}$) were obtained by electrospinning the pure 8% (w/v) P(LLA-CL) solution, so we selected the 4% (w/v) P(LLA-CL) solution as a control electrospinning solution. The solutions were placed in a 2.5 ml plastic syringe with a blunt-ended needle (inner diameter 0.21 mm). The syringe was placed in a syringe pump (789100C, Cole-Pamer Instrument Co., Vernon Hills, IL) operating at a flow rate of 1.2 ml/h. A voltage of 12 kV was generated by a high voltage power supply (BGG6-358, BMEI Co. Ltd., Beijing, China). To obtain aligned nanofibers a rotating drum collector was used at a speed of 4000 r.p.m. The distance between the needle and the collector was 12–15 cm (Fig. 1). The SF/P(LLA-CL) nanofibrous scaffolds obtained were placed in a desiccator saturated with 75% ethanol vapor at 25°C for 6 h, making the scaffolds insoluble in water.

The fabrication process for the aligned NGC is outlined in Fig. 2. The aligned nanofibrous scaffold was reeled onto a stainless steel bar with a diameter of 1.4 mm and sealed with 8-0 nylon monofilament suture stitches (Shanghai Pudong Jinhuan Medical Products Co. Ltd., Shanghai, China), ensuring that the orientation of the nanofibers was parallel to the axis of the bar. The length of the

NGC was 12 mm and the inner diameter and wall thickness were 1.4 and 0.3 mm, respectively.

2.4. Structural morphology of the aligned nanofibrous scaffolds

The morphology of the aligned SF/P(LLA-CL) and P(LLA-CL) nanofibers was observed by scanning electron microscopy (SEM) (JSM-5600, Japan) at an accelerating voltage of 15 keV. The mean fiber diameters were estimated using ImageJ image analysis software (National Institutes of Health, Bethesda, MD).

2.5. In vivo nerve regeneration studies

2.5.1. Surgical procedure

In this study all experimental procedures involving animals were conducted under Institutional Animal Care guidelines and approved ethically by the Administration Committee on Experimental Animals (Shanghai, China).

Thirty-six adult male Sprague–Dawley rats weighing 200–250 g were randomly divided into three groups of 12 animals each. These

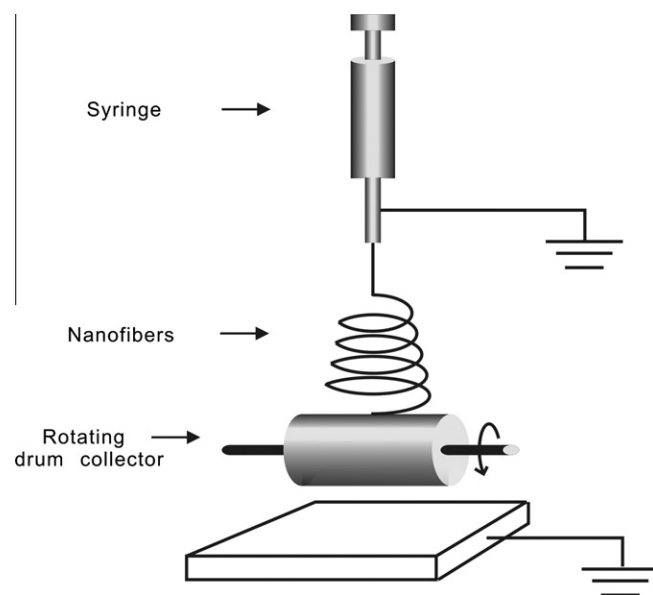


Fig. 1. A schematic illustration of the experimental set-up for fabricating aligned nanofibers.

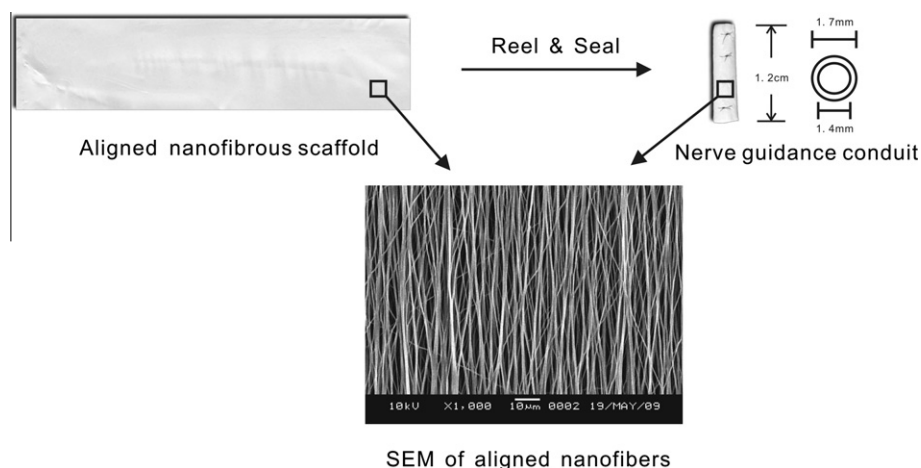


Fig. 2. A schematic illustration of the design of the aligned nerve guidance conduit (NGC). The aligned silk fibroin (SF)/P(LLA-CL) and P(LLA-CL) nanofibrous scaffolds were reeled onto a stainless steel bar and sealed with nylon monofilament suture stitches. The orientation of the nanofibers was parallel to the axis of the bar.

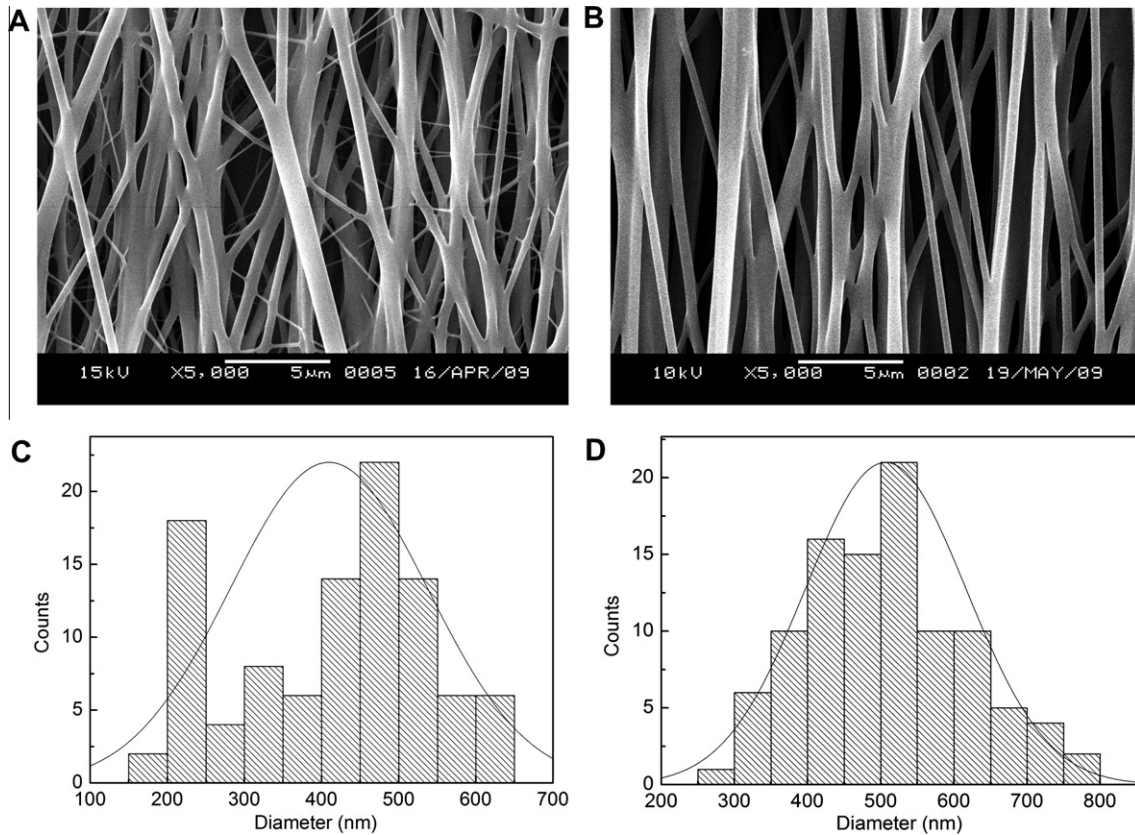


Fig. 3. SEM images and diameter distributions of electrospun SF/P(LLA-CL) and P(LLA-CL) nanofibers. (A and C) SF/P(LLA-CL) nanofibers; (B and D) P(LLA-CL) nanofibers.

groups were the P(LLA-CL) NGC (negative controls, group I), SF/P(LLA-CL) NGC (group II) and autograft (positive controls, group III) groups. All rats were anesthetized by intraperitoneal injection of 100 mg kg^{-1} ketamine and the right sciatic nerve of each animal was exposed by incision through the dorsolateral gluteal muscle. In groups I and II a 7–8 mm nerve segment was resected and removed proximal to the bifurcation of the sciatic nerve, leaving a 10 mm long defect following retraction of the nerve ends. Then a SF/P(LLA-CL) or P(LLA-CL) NGC was used to bridge the nerve defect (Fig. 4C). In group III a 10 mm nerve segment was resected, rotated 180° and re-implanted across the nerve defect. Each implant was sutured to both the proximal and distal nerve stumps with 8-0 nylon sutures. Finally, the surgical incisions were closed in a routine fashion. All animals were kept under standardized laboratory conditions in a temperature and humidity controlled room with free access to food and water.

2.5.2. Electrophysiological evaluation

The electrophysiological assessments were performed 4 and 8 weeks after implantation. Each rat was anesthetized and the NGCs in groups I and II were removed, exposing the sciatic nerve. A monopolar recording electrode and bipolar stimulating electrodes were applied to induce and record electrical activity. Nerve conduction velocity (NCV) and distal compound motor action potential (DCMAP) responses to the stimuli were recorded on a digital MYTO electromyograph machine (Esaote, Genoa, Italy).

2.5.3. Histological analysis

The morphological evaluations were performed at 4 and 8 weeks after implantation, following the electrophysiological study. Axonal regeneration was investigated by toluidine blue staining, immunohistochemistry and transmission electron microscopy (TEM) in the middle of the sciatic nerve. The samples were fixed

in 2.5% glutaraldehyde in 0.1 M phosphate buffer (pH 7.4) at 4°C for 48 h before further processing, followed by post-fixing with 1% osmium tetroxide, ethanol dehydration and embedding in Epon[®] 812 (Electron Microscopy Sciences, Hatfield, PA).

Thin, $1 \mu\text{m}$ sections were taken from each sample using a Leica EM UC6 ultramicrotome and stained with 1% toluidine blue for light microscopy. At $400\times$ magnification six random fields per nerve were evaluated with ImageJ software and morphometric indices, including the total number of nerve fibers, percent neural tissue ($(\text{neural area}/\text{intrafascicular area}) \times 100$) and myelinated axon diameter, were calculated. Parts of the sections were examined by immunohistochemistry using an antibody against S100 (1:150 dilution, Invitrogen, Carlsbad, CA) and the percent S100-positive area ($(\text{positive area}/\text{intrafascicular area}) \times 100$) of each group was calculated in a transverse section. For electron microscopy ultrathin sections of 70 nm were cut, placed on 0.5% formvar coated meshes and stained with uranyl acetate and lead citrate. The thickness of the myelin sheath was evaluated using ImageJ software.

2.6. Statistical analysis

The data are expressed as means \pm standard errors of the mean (SEM). Statistical analyses were performed using the SPSS 11.0 software package (SPSS Inc., Chicago, IL). The statistical significance of differences between groups was determined as $*P < 0.05$ and $**P < 0.01$ by LSD analysis of variance (ANOVA).

3. Results

3.1. Structure and appearance of aligned nanofibers and NGCs

The SEM morphologies and fiber diameter distributions of aligned SF/P(LLA-CL) and P(LLA-CL) nanofibers are shown in Fig. 3.

The SEM morphologies show that aligned nanofibers could be obtained using a rotating drum set-up with a 4000 r.p.m. rotation rate. In addition, the fibers had a solid surface with interconnected voids

and a porous structure. The average diameters of the aligned SF/P(LLA-CL) and P(LLA-CL) nanofibers were 409 ± 128 and 507 ± 110 nm, respectively. Although the concentration of the

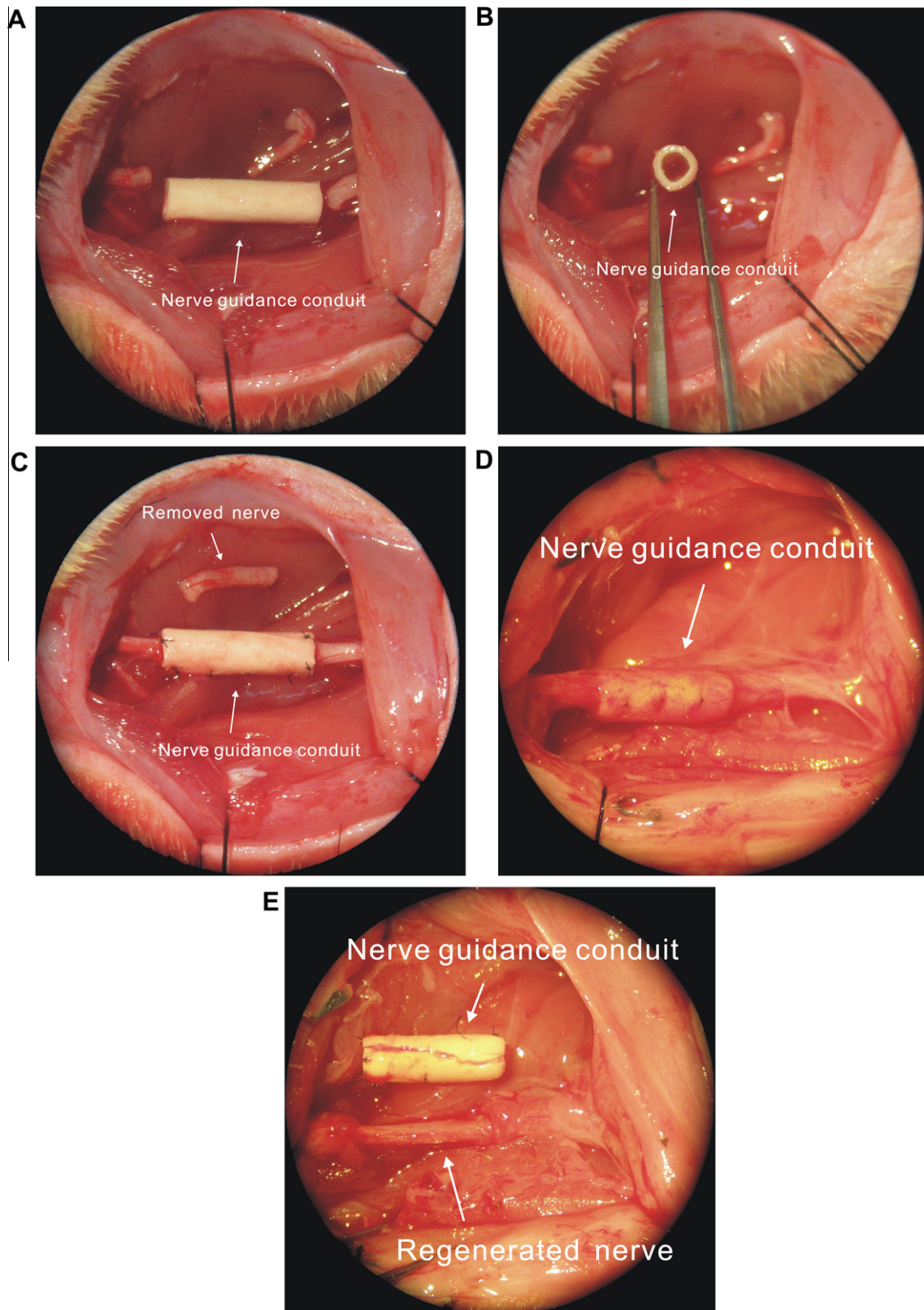


Fig. 4. Surgical implantation of the aligned NGC for nerve regeneration in a rat sciatic nerve model under a microscope (10 \times magnification). (A and B) The contour of the aligned SF/P(LLA-CL) NGC before implantation; (C) the SF/P(LLA-CL) NGC was used to bridge the 10 mm nerve defect; (D and E) the contour of the SF/P(LLA-CL) NGC 8 weeks after implantation.

SF/P(LLA-CL) solution (8% w/v) was twice that of P(LLA-CL) (4% w/v), the average diameter of the aligned SF/P(LLA-CL) nanofibers was less than that of the P(LLA-CL) nanofibers. The results show that the addition of SF decreased the nanofiber diameter. This phenomenon could be explained by the increase in conductivity of the blend solution with increasing SF content. SF is a typical amphiprotic macromolecule electrolyte, composed of hydrophobic blocks with highly preserved repetitive sequences consisting of short side-chain amino acids such as glycine and alanine and hydrophilic blocks with more complex sequences that consist of larger side-chain as well as charged amino acids [19]. When SF was affiliated, more ions were formed in the blend solution. The conductivity of the solution could increase through the addition of ions. On the other hand, the increased charge density could increase the elongational forces, resulting in the fiber jet yielding a smaller fiber [20].

Fig. 4A and B shows the contour of the aligned SF/P(LLA-CL) NGC under a microscope (10 \times magnification) before implantation. Fig. 4D and E displays the contour of the SF/P(LLA-CL) NGC under a microscope (10 \times magnification) 8 weeks after implantation. The NGC was covered by vascular fascia, indicating that the SF/P(LLA-CL) NGC had good biocompatibility. Eight weeks after implantation the NGC maintained its structure and mechanical integrity for nerve regeneration. In this study no collapse of the NGC occurred.

3.2. Electrophysiological evaluation

Both the NCV and DCMAP values gave significant information regarding the evaluation of the functional results for the regenerated nerve. Fig. 5A shows the NCV of regenerated nerves at 4 and 8 weeks after implantation. At week 4 after implantation there was a significant difference between the P(LLA-CL) ($11.75 \pm 1.20 \text{ m s}^{-1}$) and SF/P(LLA-CL) ($15.44 \pm 1.51 \text{ m s}^{-1}$) groups ($n = 6$, $P < 0.05$). By week 8 the NCV for the SF/P(LLA-CL) group ($29.25 \pm 3.27 \text{ m s}^{-1}$) was restored to a greater extent than that of the P(LLA-CL) group ($21.23 \pm 2.50 \text{ m s}^{-1}$) ($n = 6$, $P < 0.01$). However, at weeks 4 and 8 the NCV of the autograft group (21.78 ± 2.87 and $40.90 \pm 3.07 \text{ m s}^{-1}$) was better restored compared with the P(LLA-CL) and SF/P(LLA-CL) groups ($n = 6$, $P < 0.01$).

The amplitude of DCMAP at weeks 4 and 8 can be seen in Fig. 5B. At week 4 there was no significant difference between the P(LLA-CL) ($2.12 \pm 0.28 \text{ mV}$) and SF/P(LLA-CL) ($2.3 \pm 0.26 \text{ mV}$) groups ($n = 6$, $P > 0.05$). However, at week 8 the amplitude of DCMAP in the SF/P(LLA-CL) group ($8.08 \pm 0.76 \text{ mV}$) was higher than that of the P(LLA-CL) group ($6.73 \pm 0.69 \text{ mV}$) ($n = 6$, $P < 0.05$). At weeks 4 and 8 the amplitude of DCMAP in the P(LLA-CL) and SF/P(LLA-CL) groups was lower than that of the autograft group (3.75 ± 0.81 and $13.4 \pm 0.94 \text{ mV}$) ($n = 6$, $P < 0.01$).

3.3. Histological and histomorphometric analysis

Transverse sections in the middle segment of the regenerated nerve were analyzed by toluidine blue staining. As shown in Fig. 6, at week 8 post-implantation there were more nerve fibers in the SF/P(LLA-CL) and autograft groups than the P(LLA-CL) group. Additionally, the arrangement of the fibers in the SF/P(LLA-CL) and autograft groups were more “organized” compared with the P(LLA-CL) group.

Total myelinated fiber counts of the regenerated nerves, a measure of the effectiveness of neural regeneration at weeks 4 and 8 in each group, are shown in Fig. 7A. At week 4 the number of myelinated axons in the SF/P(LLA-CL) group (4506 ± 121) was significantly greater than that of the negative control (3907 ± 199) ($n = 6$, $P < 0.05$), although it was significantly less than that of the positive control (9596 ± 680) ($n = 6$, $P < 0.01$). At week 8 the number of myelinated axons in the SF/P(LLA-CL) group (6638 ± 166) was sig-

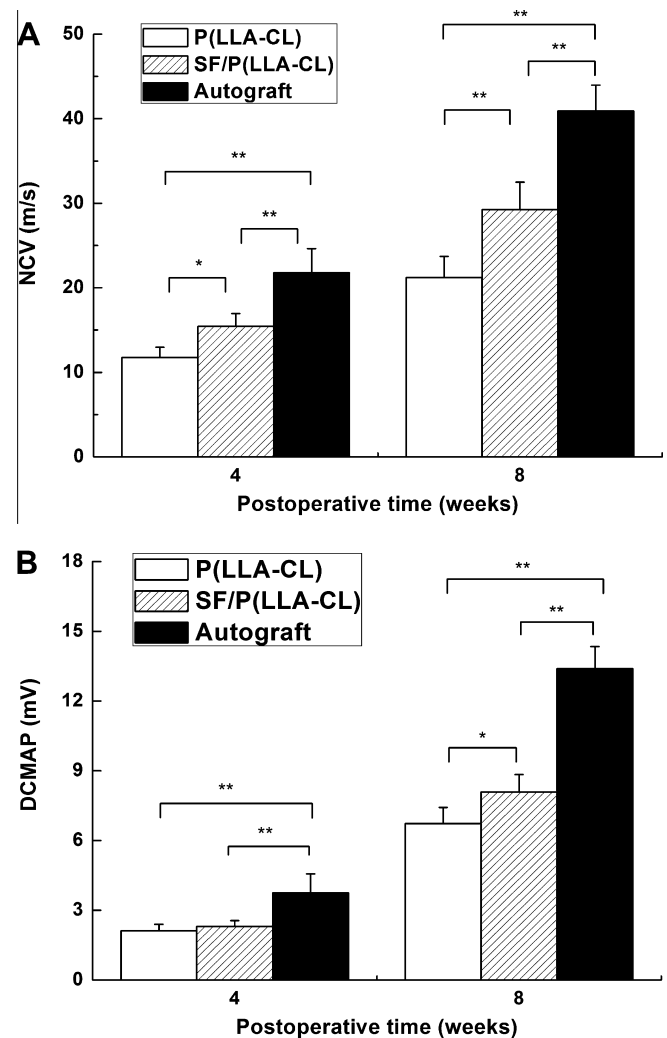


Fig. 5. Electrophysiological evaluation. (A) NCV evaluation at weeks 4 and 8 after implantation of NGCs (or autograft). (B) DCMAP evaluation at weeks 4 and 8 after implantation of NGCs (or autograft). $n = 6$, * $P < 0.05$ and ** $P < 0.01$, determined by LSD analysis of variance (ANOVA).

nificantly more than that in the negative controls (4973 ± 118) ($n = 6$, $P < 0.01$), and more than that of the two controls.

Fig. 7B shows the percentage of nerve fibers in each regenerated nerve at weeks 4 and 8. It is a parameter indicative of both the number and degree of maturity of the regenerated nerve [21]. At week 4 the percent nerve fibers in the SF/P(LLA-CL) group was $25.5 \pm 0.97\%$, and $18.53 \pm 5.73\%$ and $19.18 \pm 1.02\%$ in the negative and positive controls, respectively. At week 8 the percent nerve fibers in the negative control and SF/P(LLA-CL) groups were $24.81 \pm 3.11\%$ and $42.72 \pm 1.87\%$, respectively. Statistical analysis revealed that percent nerve fibers in the SF/P(LLA-CL) group ($25.5 \pm 0.97\%$) was significantly greater than that of the controls (negative control $18.53 \pm 5.73\%$, positive control $19.18 \pm 1.02\%$) at week 4 ($n = 6$, $P < 0.01$), and was significantly more than in the negative control at week 8 ($n = 6$, $P < 0.01$). At week 8 there was no significant difference between the SF/P(LLA-CL) and positive control (46.52 ± 0.85) groups ($n = 6$, $P > 0.05$).

The myelinated axon diameter is another measure of the maturity of the regenerated nerve fibers. Fig. 8 shows the myelinated axon diameter distribution in each group at week 8. Both the SF/P(LLA-CL) and autograft groups contained a lower number of smaller nerve fibers (2–3 μm) compared with the negative control ($n = 6$, $P < 0.01$). They also demonstrated higher percentages of

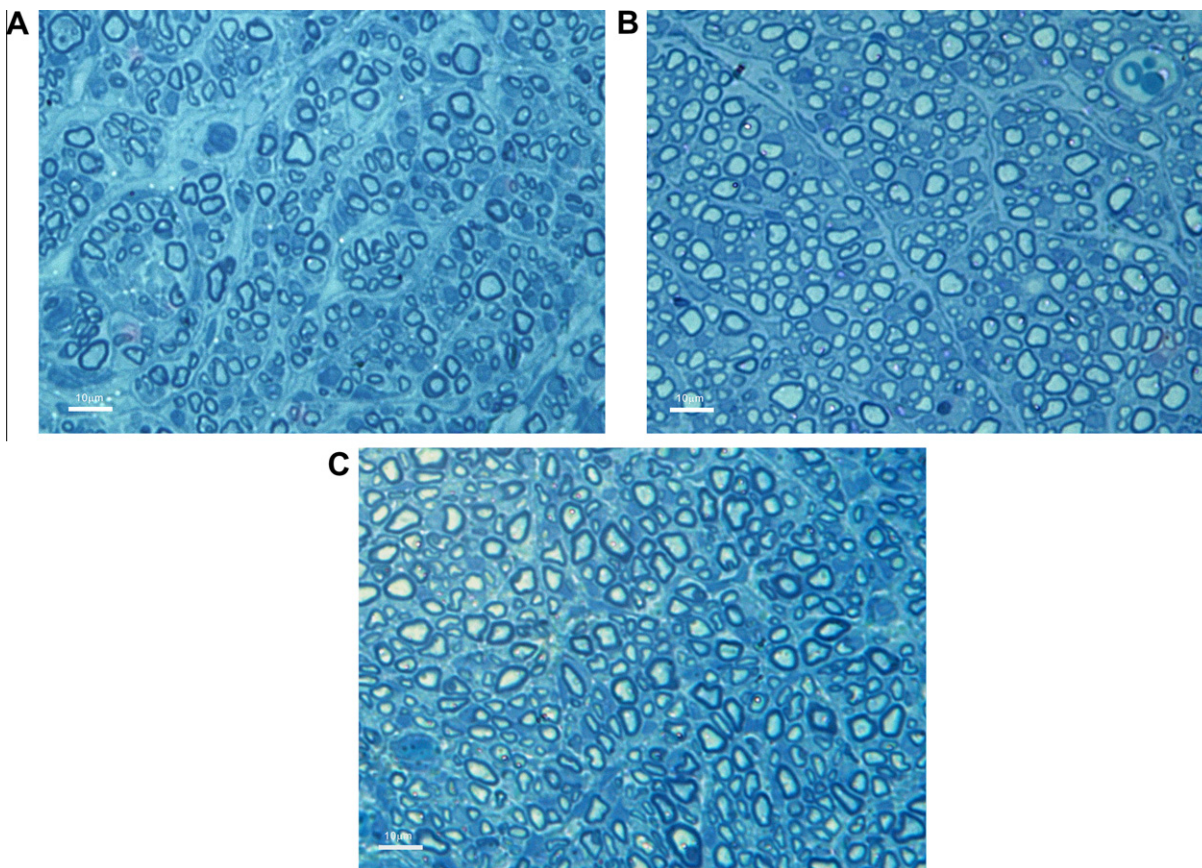


Fig. 6. Histological sections of regenerated nerves at the middle segment of the conduit (or autograft). Thin (1 μm) sections of regenerated nerve specimens were stained with 1% toluidine blue for qualitative analysis. (A) P(LLA-CL) group; (B) SF/P(LLA-CL) group; and (C) autograft group.

larger nerve fibers (3–4, 4–5 and 5–6 μm) than the negative control ($n = 6$, $P < 0.01$). There was no significant difference between the SF/P(LLA-CL) and autograft groups in terms of the percentage of larger nerve fibers (4–5, 5–6 and 6–7 μm , $n = 6$, $P > 0.05$).

3.4. Immunohistological analysis

The results of immunostaining for the Schwann cell marker S100 in transverse and longitudinal sections at week 8 post-implantation are shown in Fig. 9. As shown in Fig. 9A–F, the SF/P(LLA-CL) and autograft groups demonstrated increased levels of S100 expression and Schwann cell regeneration compared with the P(LLA-CL) group. Statistical analysis of the transverse sections revealed that the percentage S100-positive areas in the SF/P(LLA-CL) ($41.92 \pm 1.56\%$) and autograft ($47.10 \pm 1.39\%$) groups were significantly increased compared with the P(LLA-CL) group ($18.29 \pm 0.45\%$, $n = 6$, $P < 0.01$) (Fig. 9G). There was also a significant difference between the SF/P(LLA-CL) and autograft groups ($n = 6$, $P < 0.05$).

3.5. Electron microscopy

Fig. 10 shows the ultrastructure of a regenerated nerve under TEM at week 8 post-operation. The thickness of the myelin sheath was measured to indicate the maturity of the regenerated nerve fibers. Statistical analysis revealed that the myelin sheath thickness was significantly greater in the SF/P(LLA-CL) group ($0.44 \pm 0.09 \mu\text{m}$) compared with the negative controls ($0.31 \pm 0.09 \mu\text{m}$) ($n = 6$, $P < 0.01$). However, it was thinner than that of the positive controls ($0.55 \pm 0.13 \mu\text{m}$, $n = 6$, $P < 0.05$) (Fig. 10D).

4. Discussion

Recent efforts in tissue engineering in the field of peripheral nerve regeneration have been directed towards the development of NGCs. An ideal NGC should mimic the native ECM and provide temporary support for the attachment and growth of the cells. A superior NGC should also provide appropriate chemical, morphological and structural cues to direct the cells towards a targeted functional outcome [22]. In this study we have presented an aligned natural–synthetic NGC fabricated from SF/P(LLA-CL) nanofibers for peripheral nerve regeneration. The design of this NGC combines technological advances in biocompatible polymers, nanotechnology and the theory of contact guidance with significantly improved biological and mechanical properties.

SF is a natural biopolymer derived from silkworm silk and has found broad application in the pharmaceutical and biomedical fields due to its distinctive properties, such as excellent biocompatibility [23–25], biodegradability [26] and low inflammatory response induction [27]. Minoura et al. [23], reported that SF exhibited high levels of fibroblast cell attachment and growth compared with collagen, which is a component of native ECM, and the morphology of cells attached to SF was similar to those attached to collagen. Yang et al. [25], reported good biocompatibility of SF fibers with peripheral nerve tissues and cells in vitro. An in vivo study also showed that SF grafts could promote peripheral nerve regeneration [28]. However, the use of pure SF nanofiber scaffolds fabricated by electrospinning is somewhat limited due to their weak mechanical properties [18]. P(LLA-CL) is a widely used synthetic polymer which has a controllable degradation rate and unique mechanical properties [29]. However, it has limited cell

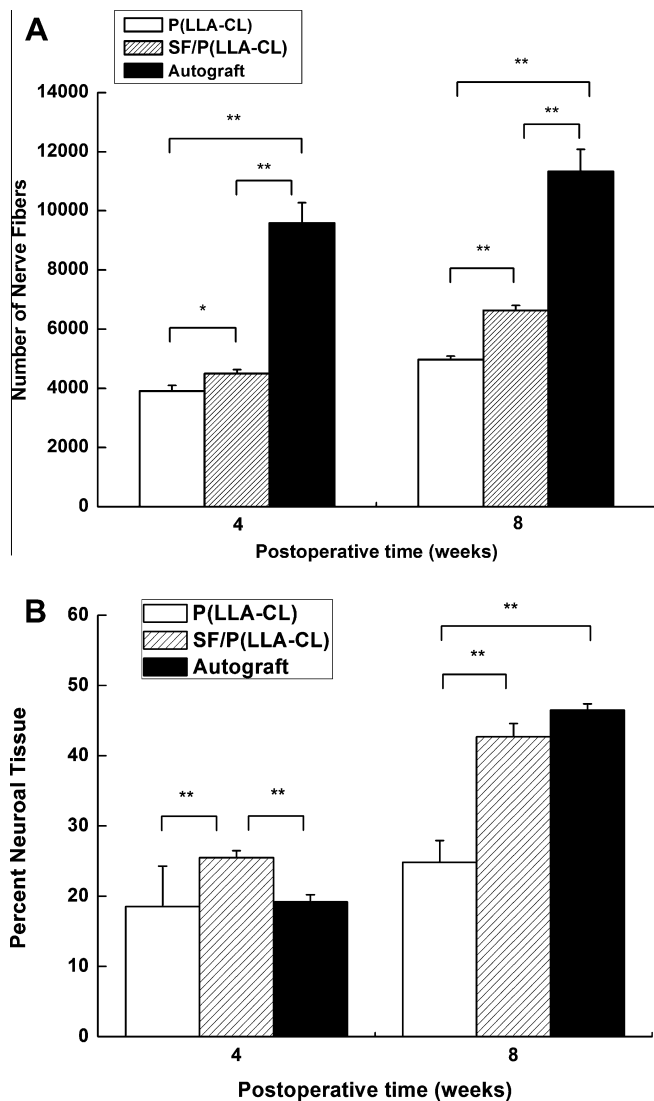


Fig. 7. Histomorphometric analysis of regenerated nerves at the middle segment of the conduit (or autograft). (A) The total myelinated fiber count of the regenerated nerve in each group at weeks 4 and 8. (B) The percent nerve fiber in each group at weeks 4 and week 8.

affinity due to its hydrophobicity and lack of cell surface recognition sites. Our previous study showed that well blended SF/P(LLA-CL) nanofibers demonstrated favorable mechanical properties and binding sites for cell attachment and proliferation, demonstrating potential application in tissue engineering [18].

With the progress in nanotechnology nanofibers have become a critical direction to consider in the field, since it is generally believed that close mimicking of the native ECM could provide a more favorable environment for cellular functions, including adhesion, migration, proliferation and differentiation [30]. We have previously fabricated ultrafine SF nanofibers by electrospinning, and an *in vitro* study has shown that these SF nanofibers were more conducive to cell attachment and growth compared with cast films [31].

The inclusion of electrospun nanofibers not only increases the total surface area available for cell growth, but also introduces contact guidance for direct cell migration. Ceballos et al. [15] reported that aligned collagen gels provided an improved template for neurite extension compared with random collagen gels. Furthermore, Chew et al. [16] found that aligned electrospun fibers could enhance Schwann cell maturation to a greater extent than random

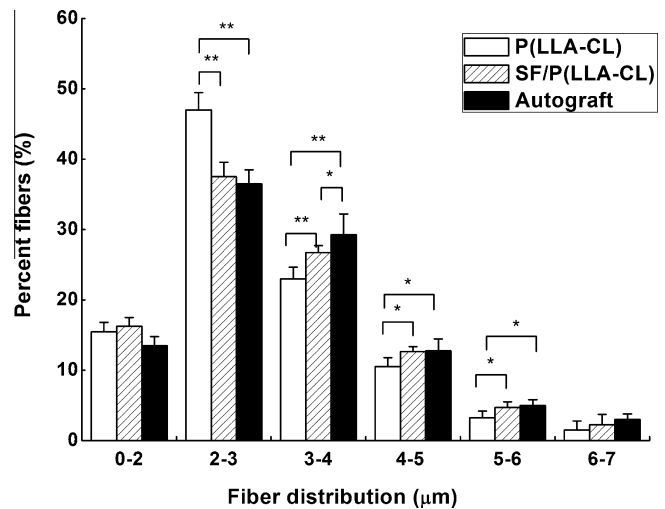


Fig. 8. The distribution of the myelinated axon diameter in the middle segment of the conduit (or autograft) at week 8. $n = 6$, * $P < 0.05$ and ** $P < 0.01$, determined by LSD analysis of variance (ANOVA).

fibers. In this study the NGC was fabricated by reeling the aligned nanofibers with the aim of introducing contact guidance along the wall of the NGC to enhance nerve regeneration.

In this study we chose a 10 mm defect in a rat sciatic nerve model, using electrophysiological, histological analysis and electron microscopy to evaluate the effect of the aligned SF/P(LLA-CL) NGC on nerve regeneration. Electrophysiological examination demonstrated significantly better restoration of NCV and DCMAP in the SF/P(LLA-CL) NGC group, indicating that functional recovery of the regenerated nerve was superior to that in the P(LLA-CL) NGC group. Histological and histomorphometric evaluation and electron microscopy indicated that the SF/P(LLA-CL) NGC group displayed better nerve regeneration in both quantity and quality compared with the P(LLA-CL) NGC group. All these results show that blending SF into P(LLA-CL) greatly enhances nerve regeneration.

There are several possible explanations. (1) Since SF protein was mainly present on the surface of SF/P(LLA-CL) nanofibers [18], blending SF protein into P(LLA-CL) actually furnished the surface of the nanofibrous scaffold with biologically active molecules. These biologically functional groups could interact with cells such as Schwann cells via cell surface receptors or initiate intracellular cell signaling pathways, which promote the formation of bands of Bünger and axonal sprouting. (2) The aligned SF/P(LLA-CL) NGC may promote the formation of blood vessels between the proximal and distal nerve stumps after injury, resulting in increased growth of the injured axon and Schwann cells compared with the P(LLA-CL) NGC. In this study the nerve conduits contained aligned nanofibers only on the inner walls. Since neurons tend to regenerate as a bundle containing hundreds of axons via the process of cofasciculation [32], directional control of a few axons within the bundle may lead to directional growth of the entire bundle [33]. In addition, aligned fibers on the inner surfaces of the NGC could provide adequate space for axonal sprouting.

Schwann cells are known as a major cellular component of peripheral nerves and have multiple crucial roles in the endogenous repair of peripheral nerves after injury [34]. S100 protein is a calcium-binding protein predominantly found in Schwann cells in the peripheral nervous system and in glia in the central nervous system. It has been reported that S100 expression in Schwann cells is related to axon diameter and degree of myelination [35]. In this study we used immunostaining for the Schwann cell marker S100 in transverse and longitudinal sections to evaluate the degree of maturity of the regenerated nerve. The percent

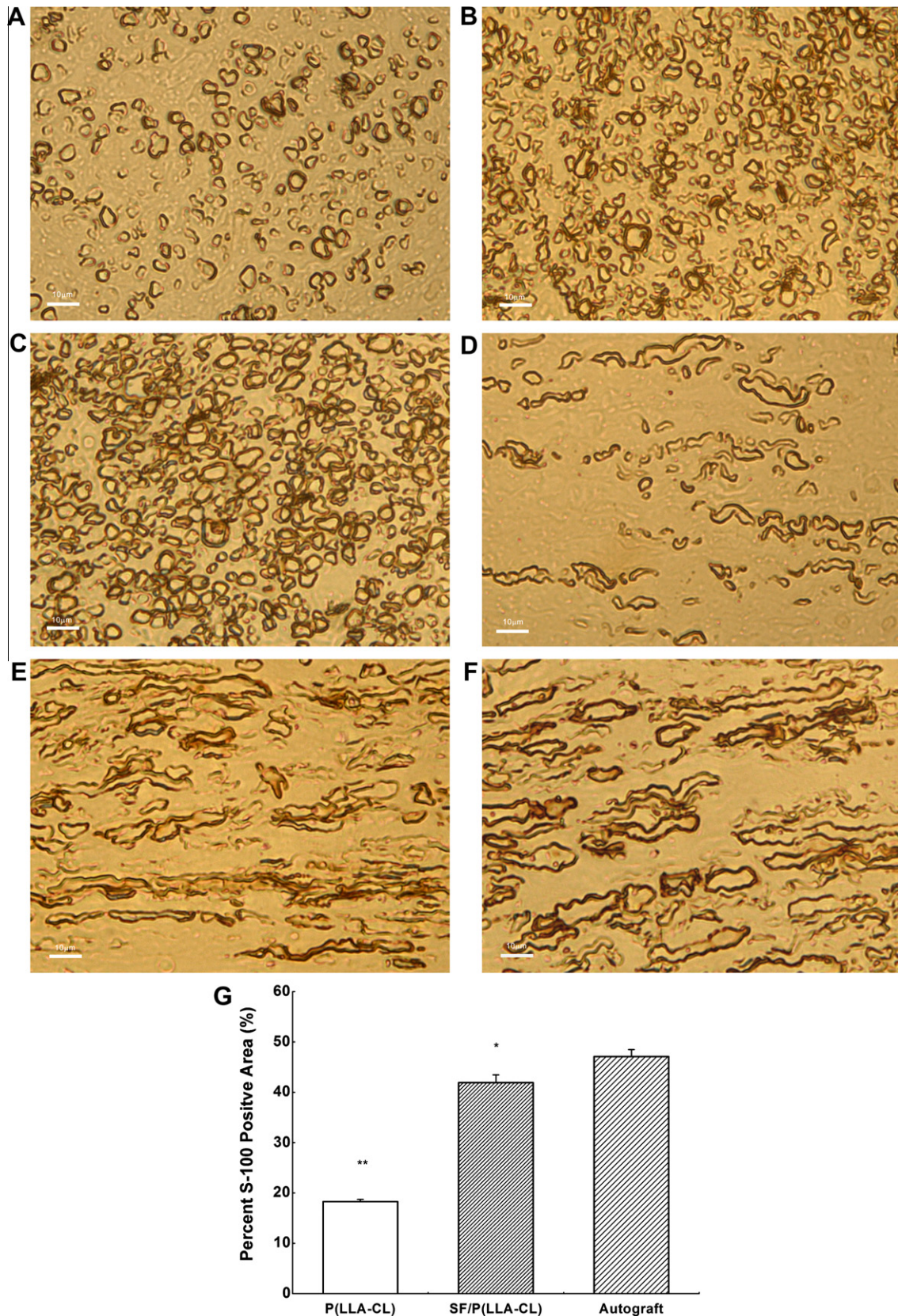


Fig. 9. Immunohistological analysis of regenerated nerves in the middle segment of the conduit (or autograft) at week 8 after implantation. (A) Transverse sections of P(LLA-CL) group; (B) transverse sections of SF/P(LLA-CL) group; (C) transverse sections of autograft group; (D) longitudinal sections of P(LLA-CL) group; (E) longitudinal sections of SF/P(LLA-CL) group; (F) longitudinal sections of autograft group. (G) The percent S100-positive area in each group. $n = 6$, $*P < 0.05$ and $**P < 0.01$, determined by LSD analysis of variance (ANOVA).

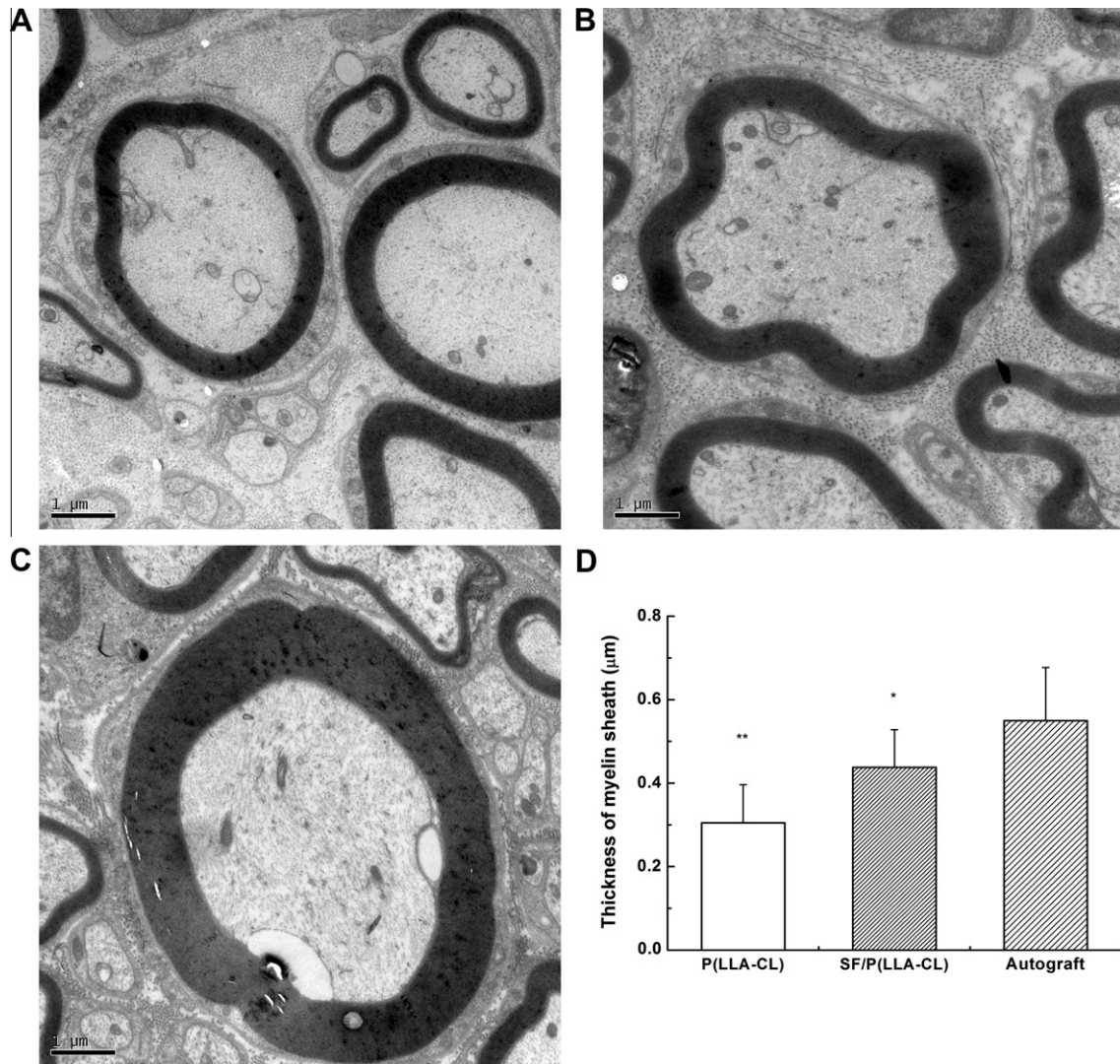


Fig. 10. Ultrastructure of the regenerated nerve under TEM at week 8 post-operatively. (A) P(LLA-CL) group; (B) SF/P(LLA-CL) group; (C) autograft group. (D) The myelin sheath thickness of each group. $n = 6$, $*P < 0.05$ and $**P < 0.01$, determined by LSD analysis of variance (ANOVA).

S100-positive area indicated that there was greater proliferation of Schwann cells in the SF/P(LLA-CL) NGC group compared with the P(LLA-CL) NGC group, which could partly explain the better nerve regeneration in the SF/P(LLA-CL) NGC group. The results also demonstrated that the outcome of nerve regeneration in the SF/P(LLA-CL) NGC group was inferior to that in the autograft group. Lacking neurotrophic factors may be one of the possible reasons. We will incorporate bioactive factors into the SF/P(LLA-CL) NGC in future research.

Biodegradability is another unique feature that should be considered in the design of NGCs. Biodegradable NGCs can provide a guide for nerve regeneration while the need for second surgical procedure to remove them can be avoided. The ideal degradation rate of NGCs should be tailored to match that of axonal sprouting [36]. Although the biodegradation properties of P(LLA-CL) and SF have been well studied individually [29,37,38], limited information has been provided with regard to that of blended SF/P(LLA-CL) nanofibers. In this study we found that the SF/P(LLA-CL) NGC could maintain its structure and mechanical integrity up to 8 weeks after implantation; further efforts should be devoted to studying the biodegradation properties of SF/P(LLA-CL) nanofibers in future.

5. Conclusions

In this study we have presented the design, processing and application of aligned SF/P(LLA-CL) NGCs for peripheral nerve regeneration. Using a critical size defect in a rat sciatic nerve model we evaluated nerve regeneration by functional and morphological analysis. All the results demonstrate that blending SF into P(LLA-CL) greatly improves nerve regeneration. Thus we believe that SF/P(LLA-CL) NGCs have potential applications in nerve regeneration.

Acknowledgements

This work was supported by grants from the Science and Technology Commission of the Shanghai Municipality Program (0852nm05000 and 0852nm03400), the Doctorial Innovation Fund of Shanghai Jiao Tong University School of Medicine (BXJ201036).

Appendix A. Figures with essential colour discrimination

Certain figures in this article, particularly Figs. 4, 6 and 9, are difficult to interpret in black and white. The full colour images can be found in the on-line version, at doi:10.1016/j.actbio.2010.09.011.

References

- [1] Meek MF, Coert JH. Clinical use of nerve conduits in peripheral-nerve repair: review of the literature. *J Reconstr Microsurg* 2002;18:97–109.
- [2] Chen MB, Zhang F, Lineaweaver WC. Luminal fillers in nerve conduits for peripheral nerve repair. *Ann Plast Surg* 2006;57:462–71.
- [3] Bellamkonda RV. Peripheral nerve regeneration: an opinion on channels, scaffolds and anisotropy. *Biomaterials* 2006;27:3515–8.
- [4] Ciardelli G, Chiono V. Materials for peripheral nerve regeneration. *Macromol Biosci* 2006;6:13–26.
- [5] Huang YC, Huang YY. Biomaterials and strategies for nerve regeneration. *Artif Organs* 2006;30:514–22.
- [6] Chew SY, Mi RF, Hoke A, Leong KW. Aligned protein–polymer composite fibers enhance nerve regeneration: a potential tissue-engineering platform. *Adv Funct Mater* 2007;17:1288–96.
- [7] Bini TB, Gao SJ, Tan TC, Wang S, Lim A, Hai LB, et al. Electrospun poly(L-lactide-co-glycolide) biodegradable polymer nanofiber tubes for peripheral nerve regeneration. *Nanotechnology* 2004;15:1459–64.
- [8] Bhattarai N, Li ZS, Gunn J, Leung M, Cooper A, Edmondson D, et al. Natural-synthetic polyblend nanofibers for biomedical applications. *Adv Mater* 2009;21:2792.
- [9] Xie JW, Li XR, Xia YN. Putting electrospun nanofibers to work for biomedical research. *Macromol Rapid Commun* 2008;29:1775–92.
- [10] Teo WE, He W, Ramakrishna S. Electrospun scaffold tailored for tissue-specific extracellular matrix. *Biotechnol J* 2006;1:918–29.
- [11] Sill TJ, von Recum HA. Electro spinning: applications in drug delivery and tissue engineering. *Biomaterials* 2008;29:1989–2006.
- [12] Schiffman JD, Schauer CL. A review: electrospinning of biopolymer nanofibers and their applications. *Polym Rev* 2008;48:317–52.
- [13] Li D, Xia YN. Electrospinning of nanofibers: reinventing the wheel? *Adv Mater* 2004;16:1151–70.
- [14] Agarwal S, Wendorff JH, Greiner A. Use of electrospinning technique for biomedical applications. *Polymer* 2008;49:5603–21.
- [15] Ceballos D, Navarro X, Dubey N, Wendelschafer-Crabb G, Kennedy WR, Tranquillo RT. Magnetically aligned collagen gel filling a collagen nerve guide improves peripheral nerve regeneration. *Exp Neurol* 1999;158:290–300.
- [16] Chew SY, Mi R, Hoke A, Leong KW. The effect of the alignment of electrospun fibrous scaffolds on Schwann cell maturation. *Biomaterials* 2008;29:653–61.
- [17] Venugopal J, Low S, Choon AT, Ramakrishna S. Interaction of cells and nanofiber scaffolds in tissue engineering. *J Biomed Mater Res B Appl Biomater* 2008;84B:34–48.
- [18] Zhang K, Wang H, Huang C, Su Y, Mo X, Ikada Y. Fabrication of silk fibroin blended P(LLA-CL) nanofibrous scaffolds for tissue engineering. *J Biomed Mater Res A* 2009.
- [19] Wang Y, Kim HJ, Vunjak-Novakovic G, Kaplan DL. Stem cell-based tissue engineering with silk biomaterials. *Biomaterials* 2006;27:6064–82.
- [20] Zong XH, Kim K, Fang DF, Ran SF, Hsiao BS, Chu B. Structure and process relationship of electrospun bioabsorbable nanofiber membranes. *Polymer* 2002;43:4403–12.
- [21] Itoh S, Takakuda K, Ichinose S, Kikuchi M, Schinomiyama K. A study of induction of nerve regeneration using bioabsorbable tubes. *J Reconstr Microsurg* 2001;17:115–23.
- [22] Zhang XH, Reagan MR, Kaplan DL. Electrospun silk biomaterial scaffolds for regenerative medicine. *Adv Drug Deliv Rev* 2009;61:988–1006.
- [23] Minoura N, Aiba S, Gotoh Y, Tsukada M, Imai Y. Attachment and growth of cultured fibroblast cells on silk protein matrices. *J Biomed Mater Res* 1995;29:1215–21.
- [24] Gotoh Y, Tsukada M, Minoura N, Imai Y. Synthesis of poly(ethylene glycol)–silk fibroin conjugates and surface interaction between L-929 cells and the conjugates. *Biomaterials* 1997;18:267–71.
- [25] Yang Y, Chen X, Ding F, Zhang P, Liu J, Gu X. Biocompatibility evaluation of silk fibroin with peripheral nerve tissues and cells in vitro. *Biomaterials* 2007;28:1643–52.
- [26] Horan RL, Antle K, Collette AL, Wang Y, Huang J, Moreau JE, et al. In vitro degradation of silk fibroin. *Biomaterials* 2005;26:3385–93.
- [27] Santin M, Motta A, Freddi G, Cannas M. In vitro evaluation of the inflammatory potential of the silk fibroin. *J Biomed Mater Res* 1999;46:382–9.
- [28] Yang Y, Ding F, Wu H, Hu W, Liu W, Liu H, et al. Development and evaluation of silk fibroin-based nerve grafts used for peripheral nerve regeneration. *Biomaterials* 2007;28:5526–35.
- [29] Meek MF, Jansen K, Steendam R, van Oeveren W, van Wachem PB, van Luyn MJ. In vitro degradation and biocompatibility of poly(DL-lactide-epsilon-caprolactone) nerve guides. *J Biomed Mater Res A* 2004;68:43–51.
- [30] Liang D, Hsiao BS, Chu B. Functional electrospun nanofibrous scaffolds for biomedical applications. *Adv Drug Deliv Rev* 2007;59:1392–412.
- [31] Zhang K, Mo X, Huang C, He C, Wang H. Electrospun scaffolds from silk fibroin and their cellular compatibility. *J Biomed Mater Res A* 2009.
- [32] Nakajima S. Selectivity in fasciculation of nerve fibers in vitro. *J Comp Neurol* 1965;125:193–5.
- [33] Rutkowski GE, Miller CA, Jęftinija S, Mallapragada SK. Synergistic effects of micropatterned biodegradable conduits and Schwann cells on sciatic nerve regeneration. *J Neural Eng* 2004;1:151–7.
- [34] Oudega M, Xu XM. Schwann cell transplantation for repair of the adult spinal cord. *J Neurotrauma* 2006;23:453–67.
- [35] Mata M, Alessi D, Fink DJ. S100 is preferentially distributed in myelin-forming Schwann cells. *J Neurocytol* 1990;19:432–42.
- [36] Zhang N, Yan HH, Wen XJ. Tissue-engineering approaches for axonal guidance. *Brain Res Rev* 2005;49:48–64.
- [37] Wang Y, Rudym DD, Walsh A, Abrahamsen L, Kim HJ, Kim HS, et al. In vivo degradation of three-dimensional silk fibroin scaffolds. *Biomaterials* 2008;29:3415–28.
- [38] Li M, Ogiso M, Minoura N. Enzymatic degradation behavior of porous silk fibroin sheets. *Biomaterials* 2003;24:357–65.